

# A Non-invasive and Automatic Ultrasound Technique for Progression Angle Measurements during Childbirth Labor

Automatic progression angle measurements through intrapartum ultrasound

## Authors:

Francesco Conversano<sup>1</sup>, Marco Peccarisi<sup>1</sup>, Paola Pisani<sup>1</sup>, Marco Di Paola<sup>1</sup>, Tommaso De Marco<sup>1</sup>, Roberto Franchini<sup>1</sup>, Antonio Greco<sup>1</sup>, Gerardo D'Ambrogio<sup>2</sup>, Sergio Casciaro<sup>1</sup>.

<sup>1</sup>National Research Council, Institute of Clinical Physiology, Lecce, Italy

<sup>2</sup>Department of Obstetrics and Gynecology, Hospital "Santa Caterina Novella", Galatina (LE), Italy

## Corresponding Author:

Dr. Ing. Francesco Conversano

Affiliation: National Research Council, Institute of Clinical Physiology, Lecce, Italy

Address and contact information: Consiglio Nazionale delle Ricerche, Istituto di

Fisiologia Clinica (CNR-IFC) c/o Campus Universitario Ecotekne, via per Monteroni, 73100 Lecce (Italy)

Tel.: +39 0832 422 312 – Fax: +39 0832 422 341 – e-mail: conversano@ifc.cnr.it

**Keywords—** *Ultrasonic imaging, intrapartum ultrasound, childbirth labor monitoring, progression angle, medical decision support.*

## ABSTRACT

**Objectives:** To evaluate the accuracy and reliability of a new ultrasound technique for a non-invasive and automatic assessment of the progression angle (PA) during childbirth labor monitoring.

**Methods:** A total of 39 pregnant women in the second stage of labor, with fetuses in cephalic presentation, underwent the conventional labor management and additional translabial echographic acquisitions. PA was measured on a total of 95 acquisition sessions both automatically by an innovative algorithm and manually by an experienced sonographer, who was blind with respect to algorithm outcomes. The results obtained from the manual segmentation were assumed as the reference to assess the actual

This article has been accepted for publication and undergone full peer review but has not been through the copyediting, typesetting, pagination and proofreading process, which may lead to differences between this version and the Version of Record. Please cite this article as doi: 10.1002/uog.17441

algorithm performance. In order to overcome the common difficulties that a sonographer may encounter in the pubic symphysis visualization, PA was measured by considering as the symphysis landmark its centroid rather than its distal point, therefore assuring a high measurement reliability and reproducibility, while still keeping objectivity and accuracy in the evaluation of labor progression.

**Results:** A strong and statistically significant correlation was found between the PA values measured by the algorithm and the reference ( $r = 0.99$ ,  $p < 0.001$ ). The good accuracy provided by the automatic method was also emphasized by the corresponding high values of the coefficient of determination ( $r^2 = 0.98$ ) and the low residual errors: RMSE =  $2^{\circ}27'$  (2.1%). The global agreement between the two methods, assessed through Bland-Altman analysis, resulted in the negligible average difference of  $1^{\circ}1' \pm 4^{\circ}29'$  (bias  $\pm 2$  SDs).

**Conclusions:** The proposed automatic algorithm proved to be a reliable technique for PA evaluation during childbirth labor monitoring. This innovative ultrasound approach has the potential to reduce both invasiveness and possibility of human errors with respect to currently employed methods for labor progression assessment, representing also a decision taking support for gynecologists and midwives.

## INTRODUCTION

Intrapartum assessment of labor progress is currently performed through highly subjective and invasive transvaginal manual inspections, whose inaccuracy has been widely reported in literature <sup>1-6</sup>. In fact, scientific evidences state that manual examinations are affected by high error rates (up to 88% of cases) in the determination

of labor progression parameters such as fetal head station, cervical dilatation and fetal head position <sup>2,6-10</sup>.

Therefore, childbirth labor management needs new approaches and guidelines to rely on, exploiting objective indications for standardized quantitative monitoring and appropriate medical decision taking for an early and correct identification of the most appropriate mode of delivery.

Recent papers demonstrated the ability of ultrasound (US) techniques in the measurement of labor progress parameters <sup>8,11-18</sup>. For instance, the evaluation of the “progression angle” (PA) by transperineal US imaging provides an objective, accurate, and reproducible method for determining fetal head progression during labor <sup>14,19</sup>. The estimation of PA could be useful also for the management of term pregnancies <sup>8,20</sup> and for predicting the delivery mode <sup>15,21</sup>. Nevertheless, the routine employment of these methods is currently hindered by the absence of fully automatic and objective approaches aimed at real-time support of clinical decisions.

In this context, a real-time tracking algorithm for non-invasive and automatic monitoring of PA during the second stage of labor was developed by our research group and preliminarily tested on both a birth simulator and a few parturients <sup>22,23</sup>.

Aim of the present study was to introduce an improved version of our algorithm and to evaluate its accuracy in a clinical routine context.

## **METHODS**

### **Patients**

The study was conducted at the Department of Obstetrics and Gynecology of "Santa Caterina Novella" Hospital (Galatina, Lecce, Italy) and included all the patients fulfilling the following enrollment criteria: singleton pregnancy at term gestation (37 weeks or more), fetus in cephalic presentation in the second stage of labor, absence of documented fetal malformations, absence of previous Caesarean sections, absence of contraindications to vaginal birth, uncomplicated pregnancy, and absence of severe obesity of the pregnant woman. The enrolled parturients were recruited in 2 months (from February 1<sup>st</sup> to March 31<sup>st</sup>, 2016) and all of them underwent the conventional labor management, according to standard local procedures. Additional translabial echographic acquisitions performed after uterine contraction, as detailed in the next paragraphs. Finally, the type of delivery of each patient was recorded in our database for a preliminary study of possible correlations between the values of echographically measured parameters and delivery mode. The study protocol was approved by the hospital ethics committee and all patients gave informed consent.

### **US system and acquisitions**

US acquisitions were performed employing the "SensUS Touch" system (Amolab Srl, Lecce, Italy; [www.amolab.it](http://www.amolab.it)), an echographic device consisting of a tablet PC equipped with a convex transducer operating at the nominal frequency of 3.5 MHz. The device was provided in an "open" configuration for research purposes, specifically allowing the possibility of integrating our novel software algorithm dedicated to real-time monitoring of childbirth labor through the fully automatic calculation of PA from intrapartum echographic images. However, for the present observational study, in order

to avoid any possible interference with labor management decisions, the real-time image analysis was disabled and replaced by an off-line processing of the acquired images.

Each parturient underwent a series of translabial echographic acquisitions. All the acquisitions were performed during the second stage of labor at different head stations, within 1 minute after the peak intensity of a uterine contraction. The first echographic scan was performed as soon as the patient entered the labor room (typically at the beginning of the second stage), therefore the total number of echographic acquisitions performed on a given patient depended on the fetal head station at the time of the first acquisition and the total duration of the second stage. In particular, a higher number of echographic scans was performed on the patients that were in the early second stage of labor when the monitoring was started, whereas fewer scans were performed on those who were already in the late second stage of labor, close to the delivery. The time interval between two different echographic acquisitions on the same patient was variable and always established by the clinical staff, which aimed to monitor fetal head progression by ultrasound. An ultrasound acquisition was performed each time the clinician needed to visualize the head progression.

For each acquisition, the operator placed the probe longitudinally in the translabial area, aiming to simultaneously visualize the pubic symphysis horizontally in the upper central part of the image and the fetal head edges in the underlying part, as shown in Fig. 1. In order to facilitate the operator, an ellipsoidal guide for the correct positioning of the pubic symphysis in the echographic field of view was also displayed on the system interface. Once the correct visualization was achieved, the operator started a 5-s acquisition: 100 B-mode images were acquired (frame rate  $\sim 20$  fps) and stored for the subsequent off-line analysis, in which each echographic image was analysed by the

automatic algorithm. The results provided by the automatic algorithm were finally compared with those obtained through the manual identification (i.e., segmentation) of the reference anatomical landmark structures performed on the same images by an experienced sonographer, who was blind with respect to the algorithm outcomes and whose results were assumed as reference. Actually, as detailed later in the text, for each patient the images belonging to the first acquisition session were processed through an automatic segmentation algorithm, whereas a different algorithm based on automatic pattern tracking was employed for the subsequent sessions. Anyway, both the algorithms were fully automatic and each time processed all the 100 images belonging to the considered acquisition session, finally selecting for each session a single representative image (reference image) that was also manually analyzed by the experienced sonographer in post-processing.

#### **PA definition and preliminary studies**

According to Barbera *et al.*<sup>14</sup>, PA is defined as the angle between the longitudinal axis of the pubic symphysis and the line running from the anterior edge of the pubic symphysis tangentially to the leading edge of the fetal skull. In the present work, in order to increase reliability and reproducibility, PA measurements were realized considering the pubic symphysis centroid rather than its distal point as symphysis landmark, since it is a more stable marker, easier to be detected. As a consequence, the resulting PA was the angle between the longitudinal axis of the pubic symphysis and the line running from its centroid tangentially to the leading edge of the fetal skull. Technically, the centroid is defined as the point corresponding to the “center of mass” of the pubic symphysis and it can be analytically identified through a calculation that

takes into account the locations of single symphysis pixels and their intensity values. From a practical point of view, the centroid can be easily identified with optimal accuracy by an operator as the center of symmetry of the brightest symphysis area on the image. In our case, the choice of adopting the centroid as anatomical landmark in the place of the distal point was actually motivated by two reasons: 1) the difficulties commonly encountered by the operators in the correct visualization of the anterior edge of the pubic symphysis in the acquired images, which partially limit reliability and reproducibility of PA measurements; 2) in order to implement a fully automatic algorithm for PA calculations characterized by a high reproducibility, the centroid represents a better option with respect to the distal point, since it is always located into an easily detectable high brightness bone area, whereas the distal point, which is located on the symphysis border, often presents a grey level value very close to the background noise. Fig. 2 shows an example of a typical B-mode echographic image acquired during a patient scan in which the pubic symphysis distal point is not clearly visible, whereas the centroid is detectable with a good confidence level through the previously described procedures.

The fact that the centroid is an easier point to be detected was verified through a dedicated preliminary study conducted on 10 volunteers satisfying the same enrolment criteria described in the “Patients” paragraph. An experienced sonographer acquired three translabial echographic images on each volunteer, corresponding to three different head stations, for a total of 30 different images. Then, five identical copies of each image were considered and the resulting 150 images were ordered in a random sequence. Afterwards, a different experienced sonographer was asked to mark on each image the symphysis centroid and the distal point or, in case, to declare that one or both of these

points were not visible in the image. For each group of 5 identical images, the average centroid position was calculated as the average of the 5 centroid positions marked in the single images and the same was done for the distal point. Finally, the distance between each single marked point and the corresponding average point was calculated. The single marked points whose distance from the corresponding average point was less than 2 mm were labelled as “correctly identified”, since we assumed that the average of five positions indicated by an experienced operator should be a good approximation of the “ground truth” (i.e., the actual position of the searched point). Furthermore, the mean distance between single marked points and the corresponding average point was assumed as a measure of the reproducibility of point identification.

It is important to underline that the choice of selecting the pubic symphysis centroid as a marker should not affect the accuracy of childbirth progression monitoring, because it is assessed through the temporal evolution of PA value between two or more measurements regardless of single values.

#### **US data analysis for the calculation of PA values**

The off-line analyses of acquired images were conducted through the mentioned fully automatic algorithm, which exploited a combination of morphological filters and pattern recognition methods to identify the pubic symphysis and the fetal head and to calculate the PA value. It is important to specify that neither manual corrections nor human input of any kind were applied in any step of the automatic algorithm calculations.

*Algorithm working principle.* The schematic illustration of the algorithm working principle is shown in Fig. 3. Each acquisition session, consisting of a sequence of 100 frames acquired in 5 s, was processed through the following steps:

1. *Preliminary image validation*, based on gray level and geometrical feature analysis, in order to verify the image suitability for the subsequent processing steps and to discard the images of insufficient quality;
2. *Search for raw bone structures*, based only on pixel cluster positions and their gray value intensities. The term “raw” indicates that this first attempt of marker segmentation could be somehow inaccurate because the pixel clusters identified may contain some imperfections due to noise;
3. *Pubic symphysis and fetal head detection*, based either on morphological filters for automatic identification of the landmark bone structures (if the considered image belongs to the first acquisition session) or pattern tracking methods (if the image belongs to a subsequent acquisition session).
4. *Co-registration of coordinates for pubic symphysis and fetal head*, aimed at the knowledge of the mutual position of the identified markers.
5. *PA calculation*, adopting the previously reported PA definition.

Once the described process has been iterated on all the images belonging to the considered acquisition session, the obtained results were used to select a single image representative of the whole session (reference image). The reference image selection followed the criteria reported herein: the reference image of the considered session was the image whose associated parameters (PA, symphysis centroid coordinates, fetal head centre coordinates, fetal head radius) were the closest to the corresponding average values.

*Automatic identification of landmark structures.* For each image of the considered acquisition session, the algorithm achieved the fully automatic identification of the bone structures through the steps reported in the following sub-paragraphs, according to the related indicated criteria. In particular, a custom-developed automatic segmentation approach was applied to the images of the first acquisition session, while a pattern tracking algorithm was specifically implemented for the images belonging to the subsequent acquisition sessions, in order to optimize computational resources and calculation times.

*Automatic Segmentation (applied only to the images of the first acquisition session; single steps are detailed in Appendix A).*

1. *Bone structure detection:* Bone structure landmarks (pubic symphysis and fetal head) were first identified in a preliminary manner, according to their position in the echographic image and their pixel intensities. The image was then converted into a binary map (Fig. 4a and Fig. 5a-b).
2. *Pubic symphysis segmentation:*
  - I. *Median filter application* (Fig. 4b);
  - II. *Morphological evaluations*, including selective thresholding based on geometrical distribution of white pixel clusters (Fig. 4b);
  - III. *Structure holes filling* (Fig. 4c); This morphological operation performs the “holes filling” for the identified marker, ensuring that all the pubic symphysis pixels that were erroneously excluded from the reference structure in the previous steps now correctly belong to the identified marker;

- IV. Centroid detection, using the original echographic image masked by the obtained binary map (Fig. 4d);
- V. Longitudinal axis detection, through morphological evaluations on the segmented pubic symphysis (Fig. 4d);
3. Pubic symphysis validity check, based on global geometric considerations related to symphysis longitudinal axis orientation and possibly undetected pubis symphysis parts;
4. Fetal head segmentation:
  - I. Median filter application (Fig. 5c-d);
  - II. Morphological evaluations (Fig. 5c-d);
  - III. Structure holes filling (Fig. 5e-f);
  - IV. Merging of fetal head structures (Fig. 5g);
  - V. Detection of fetal head radius and centre coordinates, by selecting only the identified pixels that optimize the fitting of the leading edge of the fetal head with a circumference (Fig. 5h);
5. Fetal head validity check, based on geometric considerations, pixels gray level intensity values inside the identified structures and analysis of the fetal head position.

Once the described process has been iterated until all the 100 images belonging to the first acquisition session of the considered patient have been analysed, the algorithm evaluated the mutual position of the identified landmark structures (i.e., pubic symphysis centroid and fetal head) and calculated the PA value of the first acquisition session. The pixel patterns corresponding to the landmark structures identified in the first acquisition session were then used as references for the pattern

tracking algorithm employed to identify the landmark structures in the subsequent acquisition sessions, as described in the next paragraph.

Fig. 4 illustrates how the Automatic Segmentation steps are applied to the image in Fig. 1 in order to identify the longitudinal axis and the centroid of the pubic symphysis. Fig. 5 illustrates how the Automatic Segmentation steps are applied to the image in Fig. 1 in order to automatically detect the profile tracts corresponding to the fetal head. The final output of the process is shown in Fig. 6.

*Pattern Tracking (applied only to the images of the subsequent acquisition sessions; single steps are detailed in Appendix B).*

1. *Pubic symphysis identification:*

- I. *Selection of pubic symphysis candidates*, considering all the pixel clusters inside the ellipsoidal guide and above a specific threshold, which was chosen as follows: the algorithm exploited the intensity values of the pixels belonging to the pubic symphysis segmented in the first acquisition session, obtaining a new optimized threshold;
- II. *Feature extraction from pubic symphysis candidates*, providing useful attributes to characterize each candidate;
- III. *Classification of pubic symphysis candidates*, by searching among the symphysis candidates the set of features that minimizes the difference with respect to the set of reference features extracted from the pubic symphysis segmented through the Automatic Segmentation.

Once the pubic symphysis was identified by the pattern tracking method, the algorithm extracted its weighted centroid and its longitudinal axis orientation

following the steps 2-IV and 2-V of the above detailed Automatic Segmentation algorithm.

2. Fetal head identification:

- I. Selection of fetal head structure candidates, considering all the pixel clusters inside fixed image bands, in which the fetal head progresses during labor, and above a specific threshold, which was again chosen by exploiting the intensity values of the pixels belonging to the structures segmented in the first acquisition session and consequently obtaining a new optimized threshold;
- II. Feature extraction from fetal head structure candidates;
- III. Classification of fetal head structure candidates.

Once the fetal head was identified by the pattern tracking method, the algorithm determined radius and centre coordinates of the corresponding fitting circumference by following the steps 4-V of the above detailed Automatic Segmentation algorithm.

Data analyses were performed on a modern personal computer equipped with an Intel i7 Core™ i7-3610QM processor at 2.3 GHz (8 GB of RAM, 64 bits): the analysis of a single patient acquisition, including fully automatic identification of the target anatomic landmarks and PA value calculation, took about 12 s for the first session elaboration and about 8 s for each subsequent session analysis, indicating the pattern tracking as a faster approach.

### **Statistical analysis**

The obtained data were employed for the assessment of the automatic algorithm accuracy compared to the results of manual segmentations of the same images performed by an experienced operator, assumed as the reference.

The correlation between PA values resulting from expert segmentations and those calculated by the proposed automatic approach was assessed through the calculation of the Pearson's correlation coefficient ( $r$ ), the coefficient of determination ( $r^2$ ) and the RMSE (root mean square error). Furthermore, the agreement between the two methods of measuring PA values was also evaluated as recommended by Altman and Bland<sup>24</sup>, by calculating the paired difference for each measurement and by estimating the bias and 95% limits of agreement relative to the average measurement of both methods.

## RESULTS

### **Employment of the pubic symphysis centroid as a reference marker**

Our preliminary study confirmed that the pubic symphysis centroid is detectable in an easier and more reproducible way with respect to the symphysis distal point.

An experienced sonographer declared that the symphysis distal point was not clearly visible in 40 out of the 150 analyzed images (26.7%), while in the same images he always marked a point as the centroid (150/150, 100.0%). The marked point resulted "correctly identified" for all the centroids (150/150, 100.0%) and for 72.7% of the distal points (80/110). Therefore, taking into account the detection rate on the whole sequence of 150 images, we can state that the final accuracy in the identification of the symphysis distal point was 53.3% (80/150) against the 100.0% observed for the centroid (150/150).

Finally, the observed average distance between single marked points and the corresponding average point assumed as the “ground truth” was  $0.8\pm 0.4$  mm for symphysis centroid and  $1.4\pm 0.9$  mm for distal point, providing a quantitative measure of the higher reproducibility of centroid detection.

### **Automatic measurements of PA values**

A group of 39 parturients was recruited for the main study. A total of 95 echographic acquisition sessions were collected from the enrolled patients: 19 parturients underwent 3 echographic acquisition sessions, 18 parturients underwent 2 echographic acquisition sessions, whereas only 2 parturient underwent only 1 acquisition session (since the child delivery was soon after). The average duration of labor monitoring was approximately 1 hour, although it was strongly dependent on the second stage total duration and the status of labor progression when the monitoring started. The proposed method was totally non-invasive and did not create any discomfort to the pregnant women, resulting very well tolerated by all the patients also because of the short duration of echographic acquisitions. Moreover, there were no cases in which possible uncontrolled movements of the parturient during the acquisitions caused malfunctions of the algorithm. In addition, the use of intrapartum US provided sometimes a psychological benefit to the parturients, giving them the impression of receiving a more complete and advanced monitoring of the labor progression.

A strong and statistically significant correlation was found between the PA values measured by the algorithm and those obtained by the expert manual segmentation:  $r = 0.99$  ( $p < 0.001$ ). The good accuracy provided by the automatic method was also

emphasized by the corresponding high values of the coefficient of determination ( $r^2 = 0.98$ ) and the low residual errors: RMSE =  $2^{\circ}27'$  (2.1%). Figure 7 shows the scatterplot of the PA measurements provided by the two different techniques, together with the line of equality and the value of Pearson's correlation coefficient. The corresponding Bland-Altman plot is reported in Fig. 8: the overall average difference in PA measurement (expressed as bias  $\pm$  2 SDs) was  $1^{\circ}1' \pm 4^{\circ}29'$ , further confirming the optimal agreement between the two methods.

### **Correlation between PA values and delivery mode**

In the present study, all the parturients whose measured PA was greater than  $137^{\circ}$  delivered naturally, where this angle value was determined through the automatic measurements and confirmed through the manual analysis of the images performed by the experienced operator. It is interesting to note that, as discussed in detail in the next section, this finding is consistent with previous literature<sup>14,25</sup>, taking into account the offset between the PA measured from the centroid rather than from the edge of the symphysis, as detailed in the next section.

### **DISCUSSION**

Recent literature reports many echographic approaches dedicated to quantitative labor monitoring<sup>25-31</sup>. However, their clinical diffusion is typically hindered by at least one of the following limitations: (i) necessity of significant operator-machine interactions, (ii) invasiveness associated with the employment of specific devices, which cause discomfort for the patient and risks of lesions or infections<sup>32</sup>.

This study introduced a new methodology for quantitative, non-invasive and automatic PA monitoring during childbirth labor. An automatic segmentation and tracking algorithm was used to identify the reference landmarks and to evaluate the fetal head progression during the second labor stage. The validation was conducted on 95 echographic acquisition sessions, evaluating the algorithm response in comparison to the manual contouring performed by an experienced operator. A strong and statistically significant correlation was found between the PA values obtained through the two methods.

An important aspect, in order to assure measurement reproducibility and reliability, was the choice of considering the pubic symphysis centroid rather than its distal point as a landmark. Usefulness and feasibility of this choice had been demonstrated through a dedicated preliminary study: an independent expert operator analyzed 150 echographic images previously acquired on volunteers, documenting that the distal point could be adequately identified only in about half of the images, whereas the centroid was always detected on the same images. Therefore, in our case, once the operator knew that he had to place the pubic symphysis within the on-screen ellipsoidal guide, the automatic algorithm was anyway able to detect the visible portion of the target anatomic structure and to calculate its centroid. In this way the ellipsoidal guide was helpful in order to simplify and standardize the image acquisition protocol, giving a reassuring feedback to the operator and providing the automatic software with a defined and limited image area for pubic symphysis search. Possible inaccuracies in the determination of the actual centroid position were proven to be negligible, with a lower discordance between manually estimated and actual position in case of centroid ( $0.8\pm 0.4$  mm) rather than distal edge ( $1.4\pm 0.9$  mm) of the pubis. Furthermore, the

automatic algorithm, employing the analytical definition of centroid, is expected to be even more accurate than the manual identification, reducing the possible errors in centroid determination to a definitely negligible level.

Actually, the change in pubic symphysis reference point simply led to an offset in PA calculation with respect to the literature-reported definition<sup>14</sup>. This offset is a function of the centroid-distal point distance, of the head-symphysis distance and of  $\sin(PA_{distal})$ , where  $PA_{distal}$  represents PA measured with respect to the symphysis distal point. A visual comparison between the two different PA measurements is reported in Fig. 9.

Barbera *et al.*<sup>14</sup> developed a geometric model from which it was possible to associate the measured PA value with a specific fetal head station, according to the classification of the American College of Obstetricians and Gynecologists (ACOG). In particular, in the range of  $PA_{distal}$  values corresponding to the whole range of ACOG fetal head stations, the offset between PA and  $PA_{distal}$  can be estimated through the following formula:

$$PA_{offset} = \alpha * \sin(PA_{distal})$$

where  $\alpha$ , which accounts for the head-symphysis distance and the centroid-distal point distance, may be approximated to a constant equal to  $17^\circ$ . Table 1 reports the association between each specific fetal head station and the corresponding PA intervals derived from the model reported by Barbera *et al.*<sup>14</sup> and adapted to the PA calculation adopted in this work.

In this way, the data obtained through our algorithm may be exploited not only for labor progression monitoring, but also for an absolute prediction of the fetal head station and of the most probable delivery mode. In fact, the evaluation of  $PA_{distal}$  during

the second stage of labor is a widely reported method to predict the delivery mode. Ciaciura-Jarno *et al.*<sup>26</sup> analyzed  $PA_{\text{distal}}$  by performing transperineal echographic scans on 68 parturients and found a good correlation between greater  $PA_{\text{distal}}$  values and natural delivery occurrences. Their results showed that all the parturients whose  $PA_{\text{distal}}$  was greater than  $126^\circ$  delivered naturally. On the other hand, they showed that only 15% of the patients who delivered naturally were associated to a  $PA_{\text{distal}}$  lower than  $126^\circ$ . By employing a similar approach on 23 parturients, Barbera *et al.*<sup>25</sup> found that when a  $PA_{\text{distal}}$  greater than  $120^\circ$  occurred, a natural delivery followed, whereas when  $PA_{\text{distal}}$  did not exceed  $108^\circ$  the Cesarean section was performed. Kalache *et al.*<sup>15</sup> confirmed in 26 parturients that an angle of  $120^\circ$  was associated to a 90% probability of a natural delivery.

In our study, the available data regarding the correlation between the calculated PA values and the delivery mode indicated that all the parturients whose measured PA was greater than  $137^\circ$  delivered naturally and this result is in good agreement with most of the published data, since this cut-off value corresponded to a  $PA_{\text{distal}}$  of about  $123^\circ$ .

In our algorithm implementation we made a couple of simplifying hypotheses. First, we assumed that PA value did not significantly change during the 5-s echographic acquisition, which is reasonable. Second, we fitted the fetal skull with a circumference, which is not rigorously correct, but, in order to calculate the PA value, only the fetal head leading edge has to be considered and it is comparable with a circumference arc.

In conclusion, the approach presented in this paper seemed to be well tolerated by all the patients, user-friendly and operator-independent, allowing objective quantification of PA with a high level of accuracy. Therefore, the proposed technique has the potential to be introduced in clinical routine as an alternative to manual

examinations to reduce both invasiveness and possibility of human errors with respect to the current state-of-the-art methods for labor progression monitoring, representing a reliable decision taking support and reducing the rate of unnecessary Caesarean sections. Future studies will be focused on more extended clinical validations, also combined with the simultaneous measurement of other labor monitoring parameters through the same approach.

#### ACKNOWLEDGMENTS

The authors wish to give special thanks to the midwives Stella Cavalcante and Maria Rosaria Congedo for their precious help and collaboration in clinical data collection in the Labor and Delivery room at the Department of Obstetrics and Gynecology of "Santa Caterina Novella" Hospital.

#### REFERENCES

1. Olah KS. Reversal of the decision for caesarean section in the second stage of labour on the basis of consultant vaginal assessment. *J Obstet Gynaecol* 2005; **25**: 115–116.
2. Dupuis O, Silveira R, Zentner A, Dittmar A, Gaucherand P, Cucherat M, Redarce T, Rudigoz RC. Birth simulator: reliability of transvaginal assessment of fetal head station as defined by the American College of Obstetricians and Gynecologists classification. *Am J Obstet Gynecol* 2005; **192**: 868–874.
3. Buchmann E, Libhaber E. Interobserver agreement in intrapartum estimation of fetal head station. *Int J Gynaecol Obstet* 2008; **101**: 285–289.

4. Sherer DM, Abulafia O. Intrapartum assessment of fetal head engagement: comparison between transvaginal digital and transabdominal ultrasound determinations. *Ultrasound Obstet Gynecol* 2003; **21**: 430–436.
5. Dietz HP, Lanzarone V. Measuring engagement of the fetal head: validity and reproducibility of a new ultrasound technique. *Ultrasound Obstet Gynecol* 2005; **25**: 165–168.
6. Kawabata I, Nagase A, Oya A, Hayashi M, Miyake H, Nakai A, Takeshita T. Factors influencing the accuracy of digital examination for determining fetal head position during the first stage of labor. *J Nippon Med Sch* 2010; **77**: 290-295.
7. Phelps JY, Higby K, Smyth MH, Ward JA, Arredondo F, Mayer AR. Accuracy and intraobserver variability of simulated cervical dilatation measurements. *Am J Obstet Gynecol* 1995; **173**: 942-945.
8. Ahn KH and Oh MJ. Intrapartum ultrasound: A useful method for evaluating labor progress and predicting operative vaginal delivery. *Obstet Gynecol Sci* 2014; **57**: 427-435.
9. Sherer DM, Miodovnik M, Bradley KS, Langer O. Intrapartum fetal head position II: comparison between transvaginal digital examination and transabdominal ultrasound assessment during the second stage of labor. *Ultrasound Obstet Gynecol* 2002; **19**: 264-268.
10. Tutschek B, Torkildsen EA, Eggebø TM. Comparison between ultrasound parameters and clinical examination to assess fetal headstation in labor. *Ultrasound Obstet Gynecol*. 2013; **41**: 425-429.

11. Eggebø TM, Gjessing LK, Heien C, Smedvig E, Økland I, Romundstad P, Salvesen KA. Prediction of labor and delivery by transperineal ultrasound in pregnancies with prelabor rupture of membranes at term. *Ultrasound Obstet Gynecol* 2006; **27**: 387–391.
12. Henrich W, Dudenhausen J, Fuchs I, Kamena A, Tutschek B. Intrapartum translabial ultrasound (ITU): sonographic landmarks and correlation with successful vacuum extraction. *Ultrasound Obstet Gynecol* 2006; **28**: 753–760.
13. Eggebø TM, Heien C, Økland I, Gjessing LK, Romundstad P, Salvesen KA. Ultrasound assessment of fetal head–perineum distance before induction of labor. *Ultrasound Obstet Gynecol* 2008; **32**: 199–204.
14. Barbera AF, Imani F, Becker T, Lezotte DC, Hobbins JC. Anatomic relationship between the pubic symphysis and ischial spines and its clinical significance in the assessment of fetal head engagement and station during labor. *Ultrasound Obstet Gynecol* 2009; **33**: 320–325.
15. Kalache KD, Duckelmann AM, Michaelis SA, Lange J, Cichon G, Dudenhausen JW. Transperineal ultrasound imaging in prolonged second stage of labor with occipitoanterior presenting fetuses: how well does the ‘angle of progression’ predict the mode of delivery? *Ultrasound Obstet Gynecol* 2009; **33**: 326–330.
16. Ghi T, Farina A, Pedrazzi A, Rizzo N, Pelusi G, Pilu G. Diagnosis of station and rotation of the fetal head in the second stage of labor with intrapartum translabial ultrasound. *Ultrasound Obstet Gynecol* 2009; **33**: 331–336.
17. Tutschek B, Braun T, Chantraine F, Henrich W. A study of progress of labour using intrapartum translabial ultrasound, assessing head station, direction, and angle of descent. *BJOG* 2011; **118**: 62–69.

18. Torkildsen EA, Salvesen KA, Eggebø TM. Prediction of delivery mode with transperineal ultrasound in women with prolonged first stage of labor. *Ultrasound Obstet Gynecol* 2011; **37**: 702–708.
19. Dückelmann AM, Bamberg C, Michaelis SA, Lange J, Nonnenmacher A, Dudenhausen JW, Kalache KD. Measurement of fetal head descent using the 'angle of progression' on transperineal ultrasound imaging is reliable regardless of fetal head station or ultrasound expertise. *Ultrasound Obstet Gynecol* 2010; **35**: 216-222.
20. Cho GJ, Hong HR, Seol HJ, Koo BH, Hong SC, Oh MJ, Kim HJ. Use of the angle of progression on ultrasonography to predict spontaneous onset of labor within 7 days. *J Perinat Med* 2015; **43**: 185-189.
21. Jin H, Cho G, Hong H, Seol H, Ahn K, Hong S, Oh M, Kim H. Prediction of delivery mode using angle of progression, before onset of labour in nulliparous women at term. *Ultrasound Obstet Gynecol* 2014; OP07.02.
22. Casciaro S, Conversano F, Casciaro E, Soloperto G, Perrone E, Di Renzo GC, Perrone A. Automatic evaluation of progression angle and fetal head station through intrapartum echographic monitoring. *Comput Math Methods Med* 2013; ID 278978 (8 pages).
23. Casciaro S, Conversano F, Casciaro E, Soloperto G, Stark M, Perrone A. Quantitative and automatic echographic monitoring of labor progression. *Proc. IEEE Int Ultrason Symp* 2012; 2635-2638.
24. Altman DG, Bland JM. Measurements in medicine. The analysis of method comparison studies. *Statistician* 1983; 307-317.

25. Barbera AF, Pombar X, Perugino G, Lezotte DC, Hobbins JC. A new method to assess fetal head descent in labor with transperineal ultrasound. *Ultrasound Obstet Gynecol* 2009; **33**: 313–319.
26. Ciaciura-Jarno M, Cnota W, Wójtowicz D, Niesłuchowska-Hoxha A, Ruci A, Kierach R, Stępień A, Nowak A, Sodowska P. Evaluation of selected ultrasonography parameters in the second stage of labor in prediction mode of delivery. *Ginekol Pol* 2016; **87**: 448-53
27. Molina FS, Nicolaides KH. Ultrasound in labor and delivery. *Fetal Diagn Ther* 2010; **27**: 61–67.
28. Simkin P. The fetal occiput posterior position: state of the science and a new perspective. *Birth* 2010, **37**: 61–71.
29. Ghi T, Youssef A, Maroni E, Arcangeli T, De Musso F, Bellussi F, Nanni M, Giorgetta F, Morselli-Labate AM, Iammarino MT, Paccapelo A, Cariello L, Rizzo N, Pilu G. Intrapartum transperineal ultrasound assessment of fetal head progression in active second stage of labor and mode of delivery. *Ultrasound Obstet Gynecol* 2013, **41**: 430–435.
30. Nizard J, Haberman S, Paltieli Y, Gonen R, Ohel G, Le Bourthe Y, Ville Y. Determination of fetal head station and position during labor: a new technique that combines ultrasound and a position-tracking system. *Am J Obstet Gynecol* 2009; **200**: 404.e1-5
31. Luria O, Megel Y, Smakhtin D, Schwake DM, Barnea O. Method for monitoring fetal heart rate from pulsed wave ultrasound during the active stage of labor. *World Congress on Medical Physics and Biomedical Engineering*, 2009; 69-72.

32. Block J. Pushed: The Painful Truth about Childbirth and Modern Maternity Care. Cambridge, MA: Da CAPO PRESS; 2007.

### CONFLICTS OF INTEREST

F. Conversano, M. Di Paola and S. Casciaro are shareholders of Amolab S.r.l., a National Research Council Spin-off company that may or may not benefit from the results of this study.

**Table 1:** Association between each specific ACOG fetal head station and the corresponding PA intervals derived from the geometric model reported by Barbera *et al.*<sup>14</sup> and adapted to the PA calculation presented in this work.

Station	Lower angle (°)	Mean angle (°)	Upper angle (°)
-5	77	80	84
-4	85	87	90
-3	91	95	98
-2	99	102	105
-1	106	109	112
0	113	116	119
+1	120	122	125
+2	126	129	131
+3	132	135	137
+4	138	141	144
+5	145	147	150

**FIGURE CAPTIONS**

**Fig. 1.** Example of a typical B-mode echographic image acquired during the patient scan: pubic symphysis and fetal head edges are shown in the upper part and in the central part of the image, respectively.

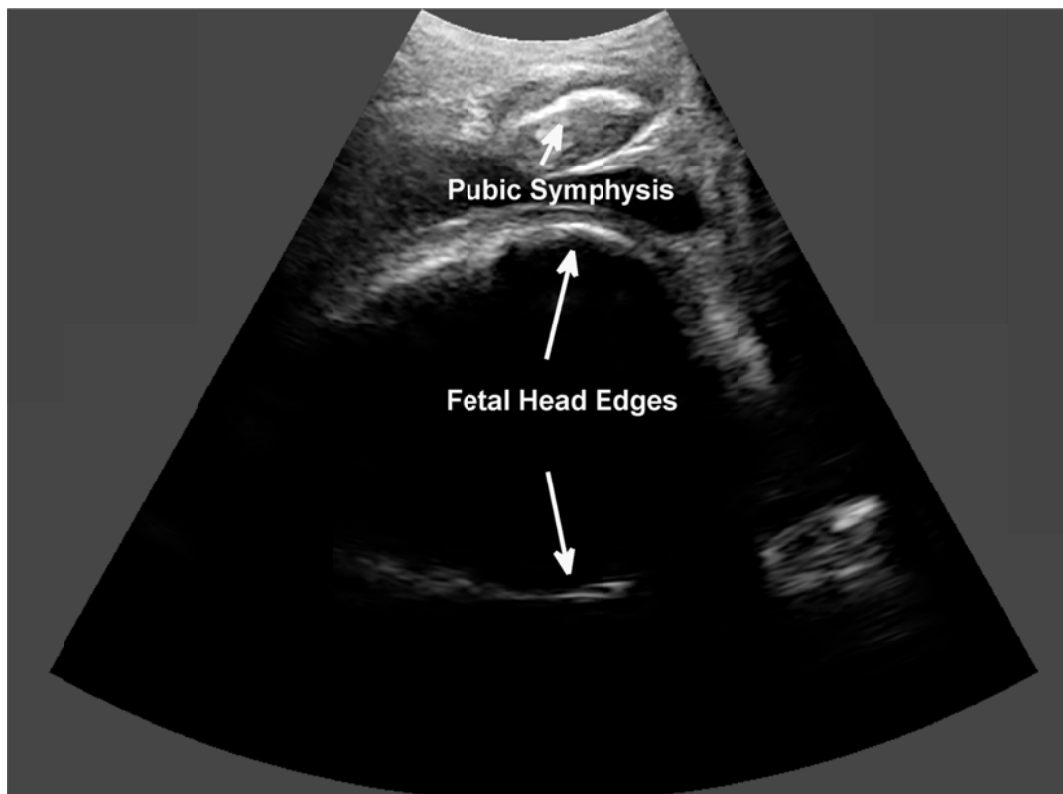


**Fig. 2.** Example of a typical B-mode echographic image acquired during a patient scan in which: (i) the pubic symphysis distal point is not clearly visible, (ii) the pubic symphysis centroid is detectable with a good confidence level through the procedure described in the text. The ellipsoidal guide for the correct placement of the symphysis within the image is also shown.

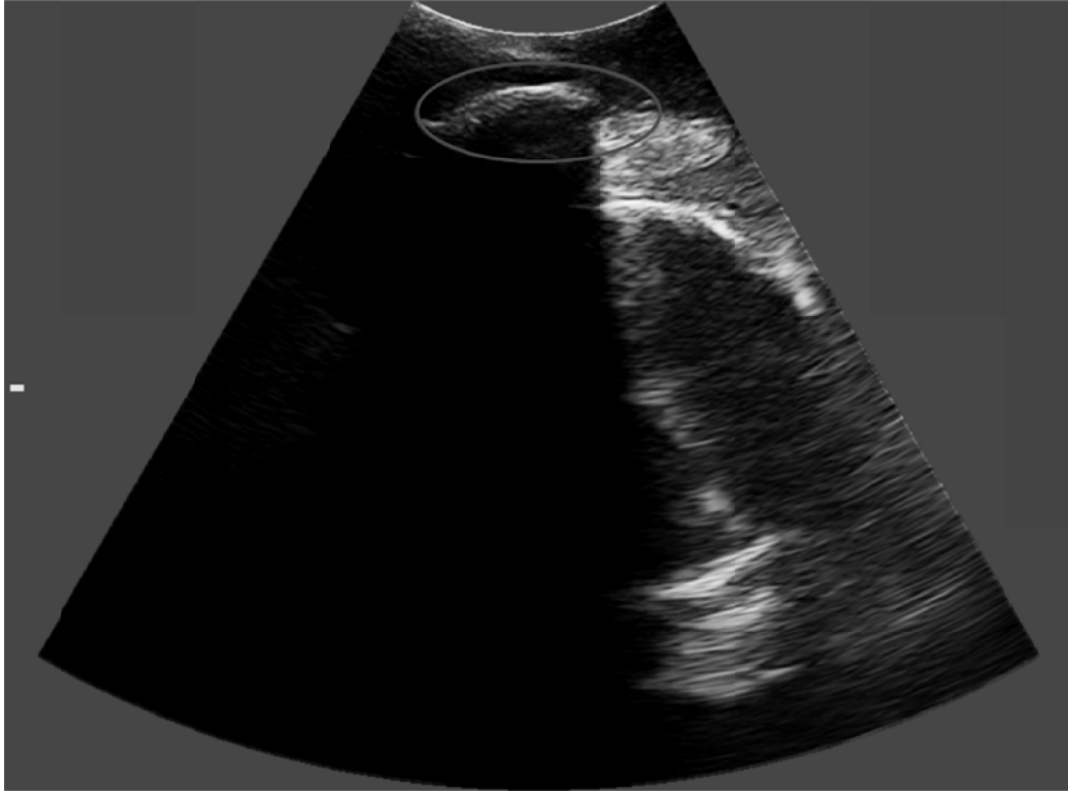


**Fig. 3.** Schematic illustration of the algorithm working principle.

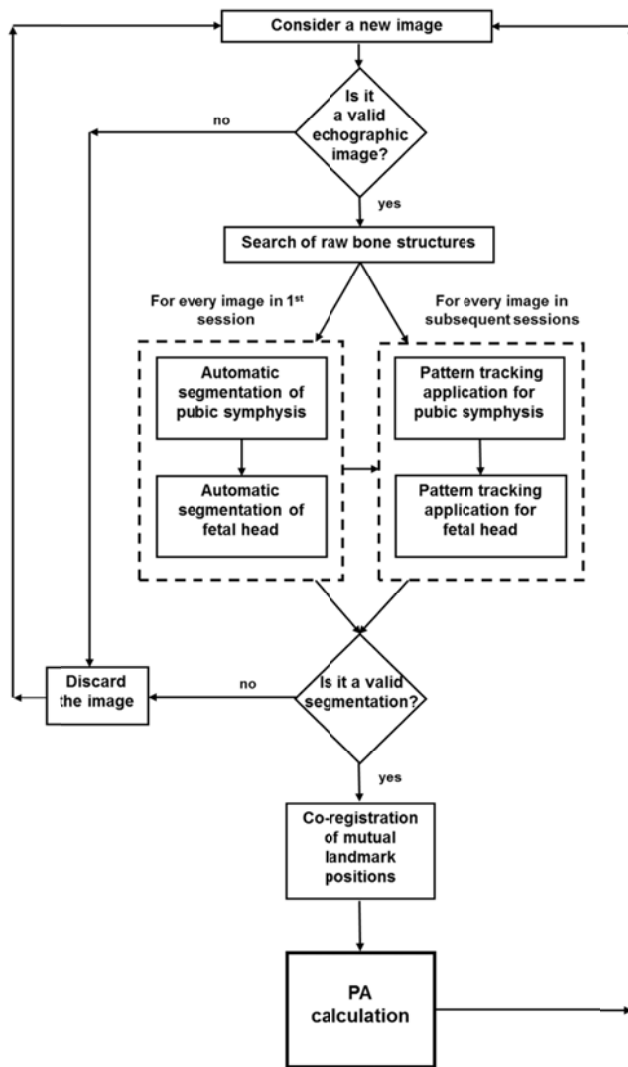


**Fig. 4.** Application of the processing steps for automatic identification of the pubic symphysis in a typical echographic image frame: a) “raw” identification of the symphysis, according to the pixel position in the image and to their gray level values, and conversion to a binary map; b) median filter application and morphological evaluations; c) structure holes filling; d) detection of pubic symphysis centroid and longitudinal axis (see Appendix A for details).

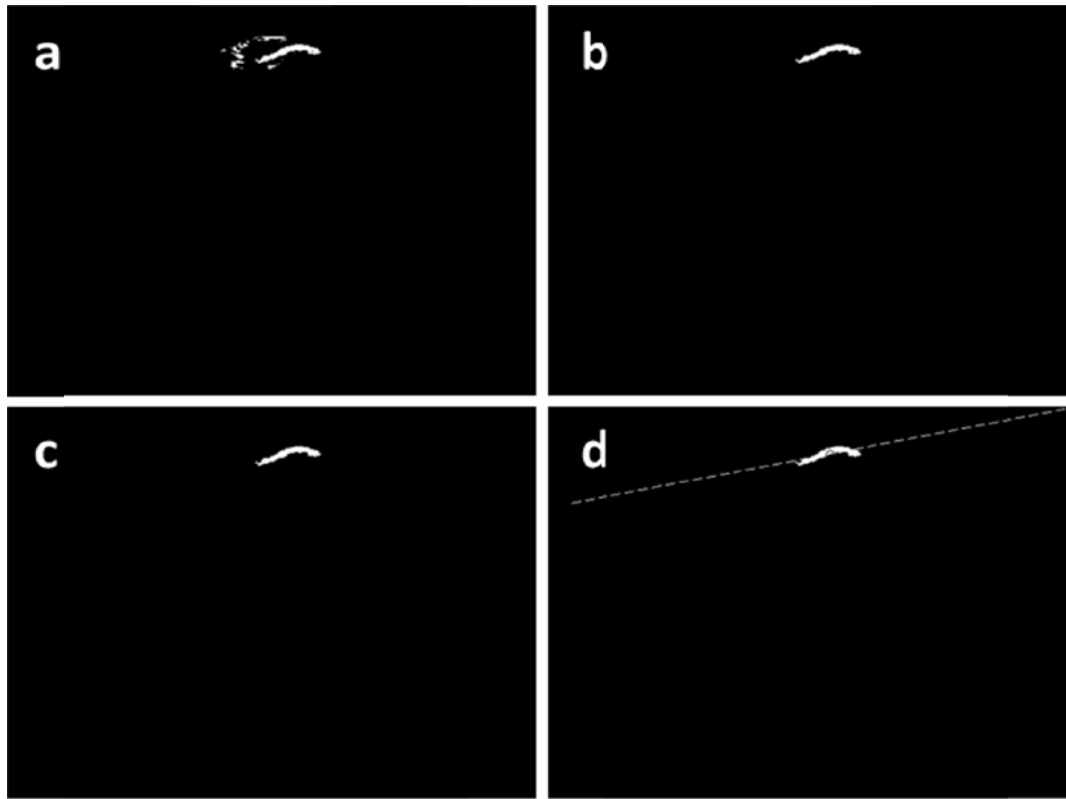


**Fig. 5.** Application of the processing steps for automatic identification of the fetal head in a typical echographic image frame: a) “raw” identification of the fetal head upper structure, according to the pixel position in the image and to their gray level values, and conversion to a binary map; b) “raw” identification of the fetal head lower structure, according to the pixel position in the image and to their gray level values, and conversion to a binary map; c) median filter application and morphological evaluations on the fetal head upper structure; d) median filter application and morphological evaluations on the fetal head lower structure; e) holes filling for the fetal head upper structure; f) holes filling for the fetal head lower structure; g) merging of fetal head structures; h) determination of fetal head centre and radius (see Appendix A for details).

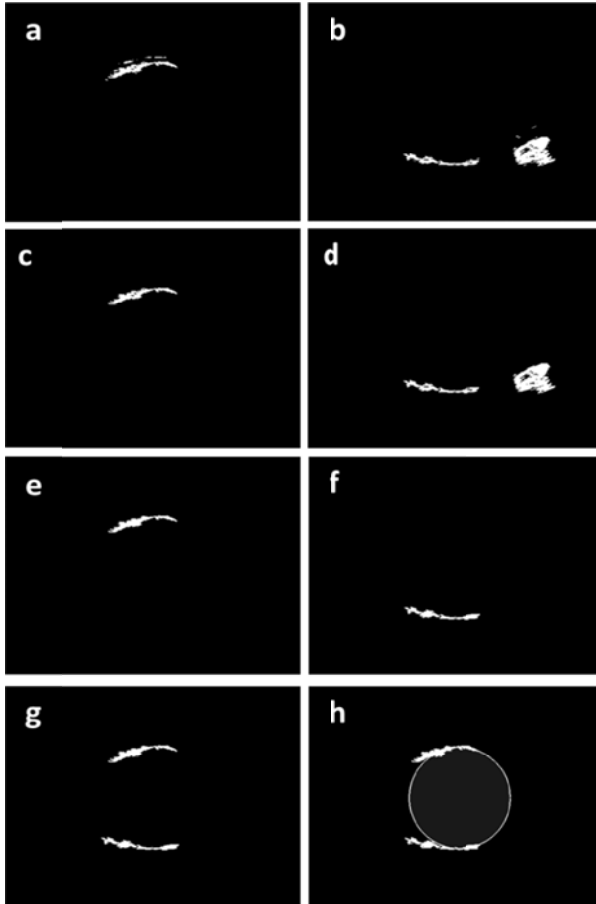


**Fig. 6.** Automatic segmentation of a typical echographic image and corresponding PA calculation.

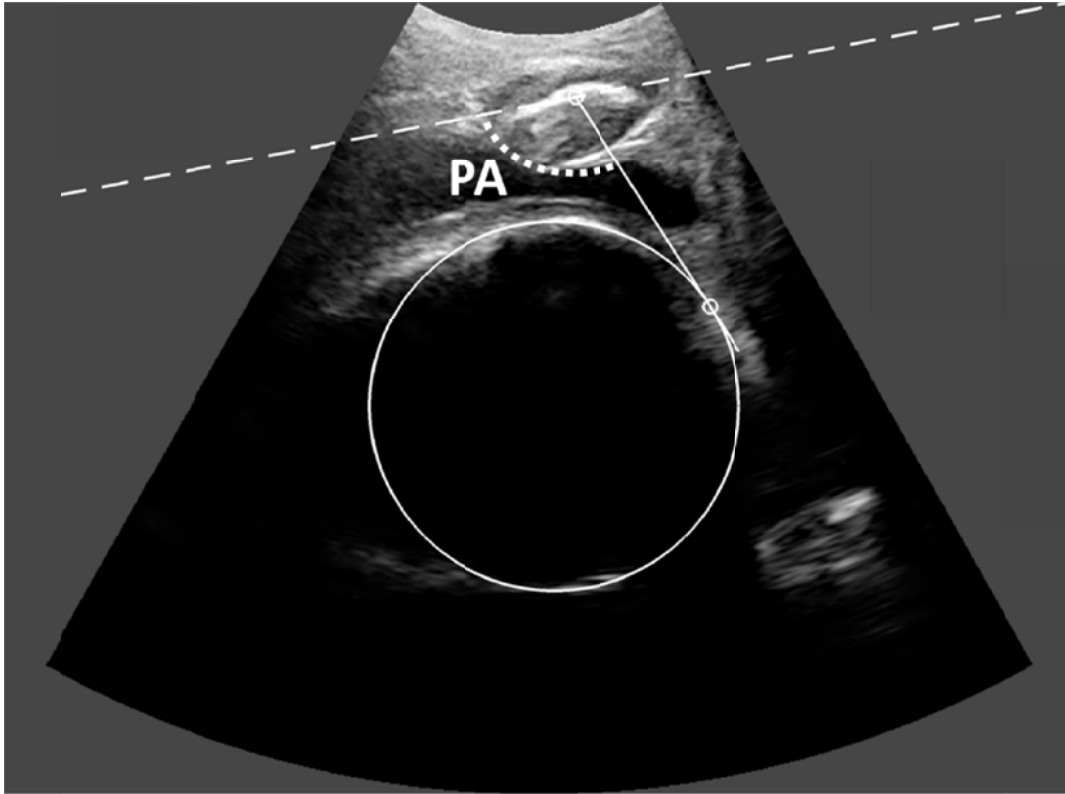


**Fig. 7.** Scatterplot of PA values provided by manual and automatic measurements. The line of equality and the global Pearson's correlation coefficient are also shown.

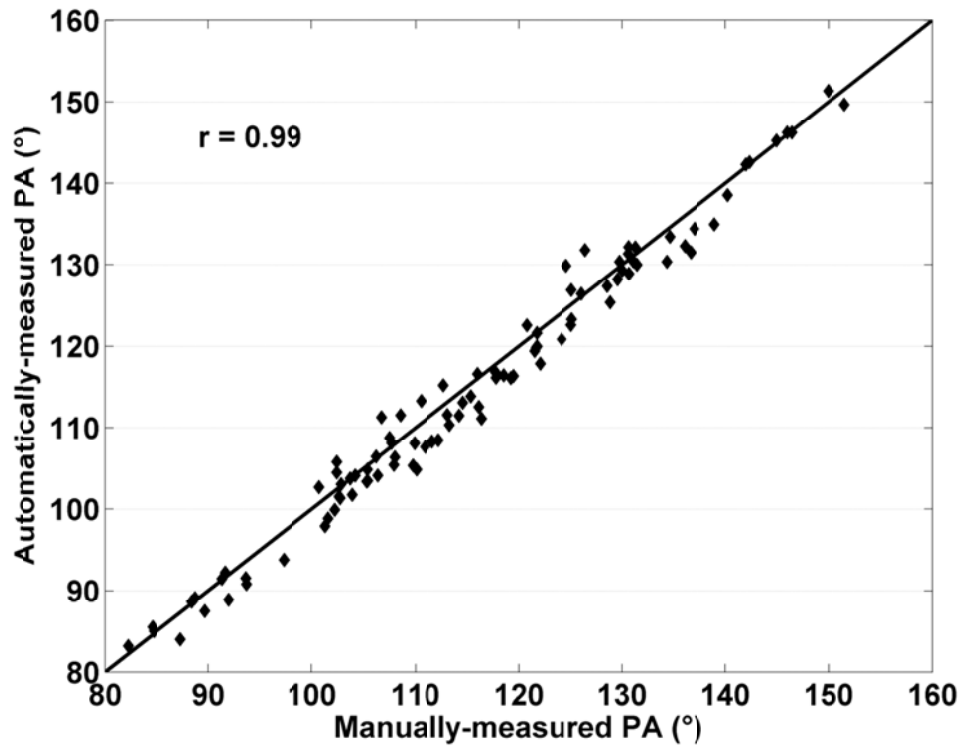


**Fig. 8.** Bland-Altman plot for the comparison of manually- and automatically-measured PA values.

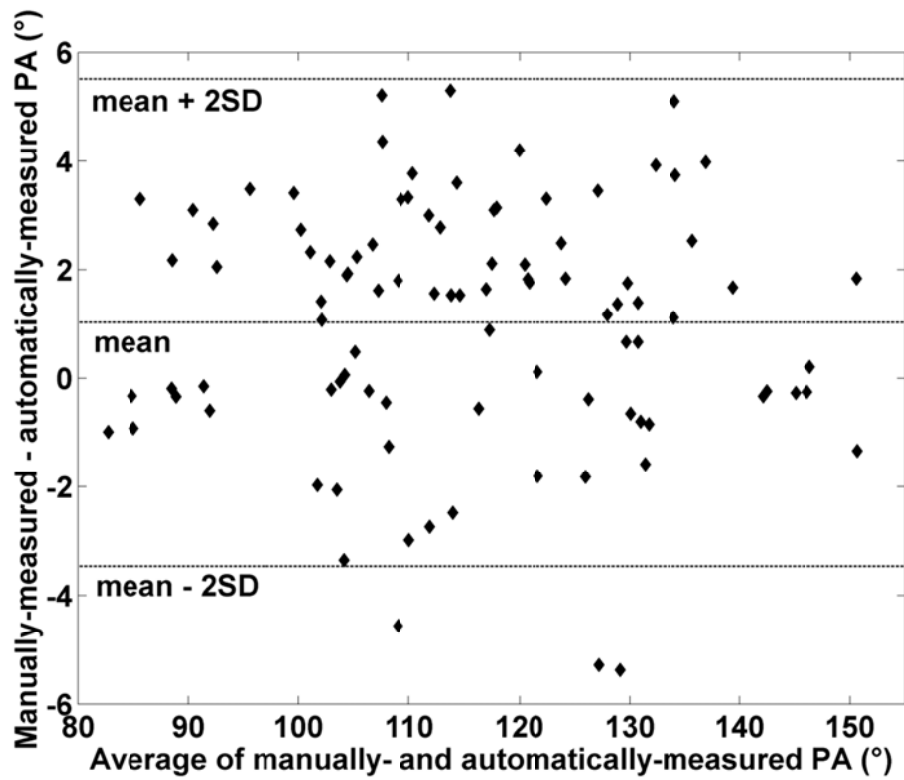
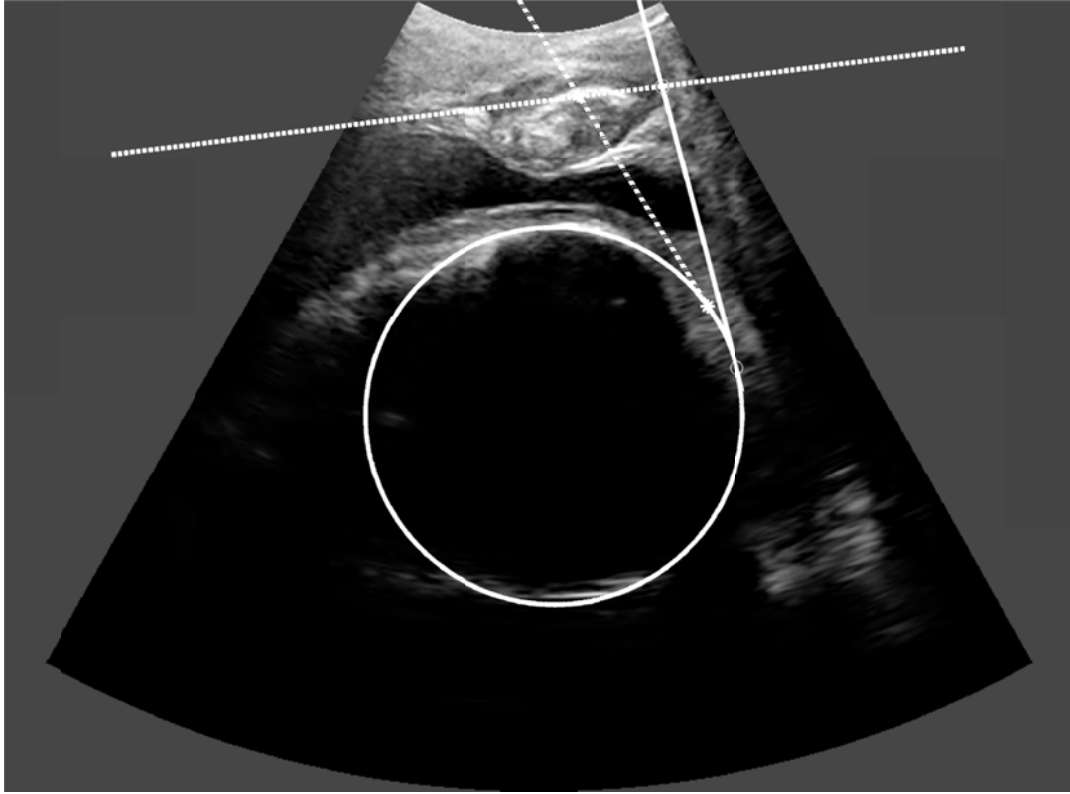


**Fig. 9.** Visual comparison between the PA measurement according to Barbera *et al.*<sup>14</sup> (angle between dashed line and solid line) and to the approach proposed in this work (angle between dashed line and dash-dot line).



## APPENDIX A

*Details of the Procedure for the Automatic Identification of Landmarks through the Automatic Segmentation (applied only to the images of the first acquisition session).*

### Automatic Segmentation.

The steps carried out on each  $i$ -th ultrasound image of the first session acquired on the considered patient for the automatic identification of the pubic-symphysis repere and fetal head structures are herein detailed:

1. Bone structure detection. Bone structure landmarks are first identified in a “raw” manner, according to their position inside the echographic image and the gray level values of their pixels. Pixels belonging to pubic symphysis are searched in the ellipsoidal guide positioned horizontally in the central part of the image at a depth ranging from 10 to 35 mm from the probe-skin interface. The considered pixels undergo a thresholding based on gray level value, in order to discriminate bone from the background. The image is then converted to a binary map (Fig. 4a). In a similar way the upper and lower edges of the fetal head are searched along two bands ranging from 35 to 75 mm and from 110 to 155 mm from the probe-skin interface, respectively. Also in this case, the considered pixels undergo a thresholding based on gray level value, in order to discriminate bones from the background and the image is then converted to a binary map (Fig. 5a-b).
2. Pubic symphysis segmentation:
  - I. **Median filter application.** This nonlinear operation is used to reduce the "salt and pepper" noise. Each pixel of the input image is replaced in the

output by a pixel containing the median value of a given neighborhood ([5x5] pixels) around the input image pixel.

- II. **Morphological evaluations.** All the clusters of white pixels representing the foreground (connected components) in the binary image are labeled. For each of the connected components, area (number of pixels of the cluster), bounding box (the smallest rectangle containing the cluster) and eccentricity (eccentricity of the ellipse that has the same second-moments as the cluster) are calculated. Quantitative cut-offs are then applied based on these parameters, starting with the selection of the only cluster of pixels that has the maximum area (above the threshold of 500 pixels) and satisfies the following criteria: eccentricity  $> 0.94$  and length of the pubic symphysis bone along its longitudinal axis in the range 20-55 mm (Fig. 4b). If no clusters satisfy the mentioned criteria, the ultrasound image is discarded and the next image in the session is considered; otherwise, the selected cluster of pixels undergoes the next step;
- III. **Structure holes filling.** This morphological operation fills the holes that may be present inside the selected cluster of pixels (pixels which were erroneously excluded from the bone structure). A hole is a set of background pixels that cannot be reached by filling in the background from the edge of the image. The aim of this operation is to select the vector of all the pixels belonging to the bone structure. Position and intensity of selected pixels are then exploited to obtain the landmark centroid (Fig. 4c);



- II. **Morphological evaluations.** The step *2-II* (above detailed) is applied to both upper and lower fetal head structures, with slight modifications of the previously defined cut-off criteria: selection of the cluster of pixels having the maximum area (above the threshold of 600 pixels), with eccentricity  $> 0.90$  and length of the fetal head structure in the range 20-120 mm (Fig. 4c-d). If there is not a cluster of pixels satisfying the mentioned criteria for each of the two considered image bands, the ultrasound image is discarded and the next image in the session is considered; otherwise, the selected clusters of pixels undergo the next step;
- III. **Structure holes filling.** The step *2-III* (above detailed) is applied to both upper and lower fetal head structures (Fig. 5e-f);
- IV. **Merging of fetal head structures.** Structures showing a coherence in position along the upper and the lower band are selected. Position coherence between upper and lower fetal head candidate structures is checked by a thresholding applied to the x-coordinate values of the bounding box of the Cartesian product of the considered clusters. The threshold is dependent from the mutual position of the structures in the ultrasound image, and is more restrictive in the central part of the image than on the side of the echographic field of view. Each couple of structures in the upper and lower band that presents coherence is selected to be fetal head structures candidate. The couple of candidates whose distance is minimal is finally chosen and the corresponding structures are merged together (Fig. 5g).

- V. **Detection of fetal head radius and centre coordinates.** The finally chosen clusters of pixels are analysed and their centroids are determined. For each identified cluster in the upper and lower band, only the pixels having  $x$ -coordinate  $>$  centroid  $x$ -coordinate are selected. These selected pixels are fitted with a circumference (Fig. 5h), assuming that the outmost part of the fetal head may be approximately fitted with a circumference arc. The corresponding circumference radius and centre coordinates are calculated.
5. *Fetal head validity check.* Aim of this step is to check whether the circumference radius and centre coordinates are within a fixed range of values. Moreover, the content of the circumference in the original analysed echographic image in terms of gray level values is evaluated: if any candidate bone structure (i.e. high gray level connected cluster of pixels) is found inside a circumference having the same centre of the fitting circumference of step 4-V and a radius reduced by 25% (in order to eliminate border noise), the image is rejected. Otherwise the algorithm stores all the information for PA calculation in the  $i$ -th parameter vector.

## APPENDIX B

*Details of the Procedure for the Automatic Identification of Landmarks through the Pattern Tracking (applied only to the images of the subsequent acquisition sessions).*

### Pattern Tracking.

The steps carried out on each  $i$ -th ultrasound image of each session acquired after the first one on the considered patient for the automatic identification of the pubic-symphysis repere and fetal head structures are herein detailed:

#### *1. Pubic symphysis identification:*

- I. **Selection of pubic symphysis candidates.** Bone structure landmarks are first identified in a “raw” manner, considering all the pixel clusters inside the ellipsoidal guide and above a specific threshold, which was chosen as follows: the algorithm exploited the pixel intensity values of the pubic symphysis pixel clusters segmented in the first acquisition session, obtaining a new optimized threshold. The image is then converted to a binary map.
- II. **Feature extraction from pubic symphysis candidates.** For each pubic symphysis candidate, a set of geometrical and first-order gray level value features is extracted. The set of geometrical features is composed by: *area* (number of pixels of the cluster), *length* (distance between the proximal and the distal points of the cluster), *border length* (number of boundary points composing the profile of the cluster), *eccentricity*

(eccentricity of the ellipse that has the same second-moments as the cluster) and *orientation* (the angle between the horizontal  $x$  axis and the major axis of the ellipse that has the same second-moments as the cluster). The first order textural features are: *pixel gray level mean*, *standard deviation*, *entropy* and *kurtosis*. Gross feature value intervals are calculated from the feature distributions and exploited for a preliminary selection of pubic symphysis candidates. If there are no pubic symphysis candidates whose feature values are in the expected intervals, the corresponding image frame is discarded.

III. **Classification of pubic symphysis candidates.** The classification is performed by searching, among the symphysis candidates, the set of features that minimizes the difference with the set of reference features extracted from the pubic symphysis segmented through the Automatic Segmentation.

2. *Fetal head identification:*

I. **Selection of fetal head structure candidates.** Bone structure landmarks are first identified in a “raw” manner, considering all the pixel clusters within two image bands respectively ranging from 35 to 75 mm and from 110 to 155 mm from the probe-skin interface and above a specific threshold, which is chosen as follows: the algorithm exploited the pixel intensity values of the fetal head pixel clusters segmented in the first acquisition session, obtaining a new optimized threshold. The image is then converted to a binary map.

- II. **Feature extraction from fetal head structure candidates.** The above detailed step *I-II* is applied to both upper and lower fetal head structures.
- III. **Classification of fetal head structure candidates.** The above detailed step *I-III* is applied to both upper and lower fetal head structures.